NJC

RSC Publishing

PAPER

View Article Online
View Journal | View Issue

Cite this: *New J. Chem.*, 2013, **37**, 2002

Synthesis, crystal structures and tautomerism in novel oximes based on hydroxyalkylpyrazolones†

Julio Belmar,*[a] José Quezada,[a] Claudio A. Jiménez,*[a] Pau Díaz-Gallifa,[b] Jorge Pasán[b] and Catalina Ruiz-Pérez[b]

Received (in Porto Alegre, Brazil) 11th February 2013,
Accepted 25th March 2013

DOI: 10.1039/c3nj00163f

www.rsc.org/njc

Two novel hydroxyethyl pyrazolones were obtained by condensation of 2-hydroxyethylhydrazine with ethyl acetoacetate or ethyl benzoylacetate, later nitrosation of the C4 carbon atom in the heterocyclic moiety, afforded two novel oxime-derivatives. The ^{1}H and ^{13}C NMR data show that 1-(2-hydroxyethyl)-3-methyl-5-pyrazolone (**1**) is largely present together with a very small amount of the 5-one tautomer in DMSO-d_6; in contrast, 1-(2-hydroxyethyl)-3-phenyl-5-pyrazolone (**2**) is found as a single tautomer in $CDCl_3$. Two diastereomers occur in DMSO-d_6 in 1-(2-hydroxyethyl)-3-methyl-4-hydroxyimino-5-pyrazolone (**3**) while in 1-(2-hydroxyethyl)-3-phenyl-4-hydroxyimino-5-pyrazolone (**4**), a single species is present in $CDCl_3$. Despite the polarity differences in the solvents used, remarkably the oxime tautomers proved to be more stable in both cases and DMSO-d_6 only allows the equilibrium between *E*/*Z* diastereomers. Single crystal X-ray diffraction data of **1**, **3** and **4** are presented, they show that **1** occurs as a keto-enamine tautomer, in clear contrast with the situation in solution; in the case of **3** and **4**, the tautomeric equilibrium remains shifted to the oximes in the solid phase as the *Z*-diastereomer, exclusively. This finding is the opposite of what was described in a previous report for 1-alkyl-3-methyl-4-hydroximino-5-pyrazolone, where the *E*-diastereomer was present. Besides, the data show that the oxime motif is not affected by the substitution changes described in C3. IR data in the solid phase supports the crystal structures and suggest that **2** occurs as a similar tautomer as **1**.

Introduction

Oxime-based ligands play an important role in several areas of chemistry. They have been widely used in analytical chemistry for separation or detection of metals[1] after Tschugaeff reported the use of dimethylglyoxime for the gravimetric determination of nickel.[2] A variety of bidentate chelating oximes are known as in the case of 2-hydroxybenzaldehyde oximes or salicylaldoximes. These kind of compounds deserve special mention because some of them are commercially available and used extensively in copper hydrometallurgy or as anticorrosives in protective coatings.[3] Almost one fifth of the total world production of copper is obtained every year in solvent extraction processes that use phenolic oximes.[3] There are however, other areas of coordination chemistry where oximes are the subject of continuous research, such as molecular magnetism,[4–6] coordination polymers and molecular clusters[5,6] or biological modeling.[5–8]

Probably the most straightforward way to obtain oximes is the condensation of a ketone or aldehyde with hydroxylamine.[9] Nitrosation reactions represent an attractive procedure to obtain oximes in the case of products that are able to undergo tautomerism such as some naphthols, phenols or ketones.[10–12] Pyrazolone oximes can also be obtained by nitrosation[13–16] and it seems that the compounds exist mainly as the oximino tautomer[16,17] in solution and in the solid phase.

The heterocycle pyrazolone has been known for years, being first reported in the 19th century by Knorr.[13] Derivatives of this heterocycle remain as the focus of continuous research. The appeal stems from the tautomerism they present[18] and from their applications in analytical chemistry in the determination of carbohydrates[19,20] or as chelating agents for a wide range of metals;[21–23] besides, they are attractive in the field of medicinal chemistry, where this moiety is often included. In daily life pyrazolones are important in dyes industry[24,25] and in medicine, where some derivatives are still used to treat pain, fever, among other diseases and symptoms[25] while other uses have appeared.[26]

[a] *Departamento de Química Orgánica, Facultad de Ciencias Químicas, Universidad de Concepción, Casilla 160-C, Concepción, Chile. E-mail: jbelmar@udec.cl, cjimenez@udec.cl; Fax: +56 41 2247954; Tel: +56 41 2204258*

[b] *Laboratorio de Rayos X y Materiales Moleculares, Departamento de Física Fundamental II, Facultad de Física, Universidad de La Laguna, Avda. Astrofísico Francisco Sánchez s/n, E-38204 La Laguna, Spain*

† Electronic supplementary information (ESI) available. CCDC 922744–922746. ESI and crystallographic data in CIF or other electronic format see DOI: 10.1039/c3nj00163f

Nitrosopyrazolones are as old as pyrazolone itself; however, they have attracted less attention than other derivatives such as acylpyrazolones, for instance. In recent years only a few reports including nitroso derivatives of the heterocycle can be found.[14,15,21,27–29] Following from our studies aimed at having a better understanding on the structural features of pyrazolones, the synthesis, structural and spectroscopic characterization of some new derivatives obtained by nitrosation are presented in this article.

Results and discussion

Synthesis and spectroscopic characterization

To date most pyrazolone derivatives reported are 1-aryl or N-1 unsubstituted derivatives. However, some of us reported years ago that 3-methyl-5-pyrazolone can be alkylated with quite good yields at the N-1 position.[30] Moreover, 3-phenyl-5-pyrazolone can also be alkylated, although the yields reported were not as good as with the 3-methyl homologue.[15] The 1-alkyl derivatives of 5-pyrazolone react with electrophiles the same way 1-aryl derivatives do and the resulting products represent interesting targets because, in general, an improved solubility in low polarity organic solvents can be expected when comparing 1-alkyl derivatives with 1-aryl homologues. Thus, encouraged by the good results previously obtained with primary and benzylic halogen derivatives[14–15,30] we focused on using hydroxylated halogen derivatives, because the resulting products would broaden scope of the alkylation of pyrazolones giving rise to new potential applications.

The first synthetic attempt considered the innovative alkylation of 3-methyl-5-pyrazolone with 2-bromoethanol, 3-bromopropan-1-ol, and 3-chloro-1,2-propanediol. This approach seemed very attractive because only a few examples of alkylhydrazines commercially available exist and the preparation of them is not straightforward.[30] Despite all our efforts, it turned out impossible to isolate any product from the reacting mixtures. No trials with 3-phenylpyrazolone were carried out since this compound is less reactive toward alkylation and a lower yield has been reported.[15] Therefore, the typical condensation of a β-keto ester with a monosubstituted hydrazine was used instead.[31] In this way (see Scheme 1), after the condensation of ethyl acetoacetate and ethyl benzoylacetate with 2-hydroxyethylhydrazine, 1-(2-hydroxyethyl)-3-methyl-5-pyrazolone (**1**) and 1-(2-hydroxyethyl)-3-phenyl-5-pyrazolone (**2**) were obtained. In the second step these compounds were treated with HCl and then with sodium nitrite, affording 1-(2-hydroxyethyl)-3-methyl-4-hydroxyimino-5-pyrazolone (**3**) and 1-(2-hydroxyethyl)-3-phenyl-4-hydroxyimino-5-pyrazolone (**4**) in good yields.

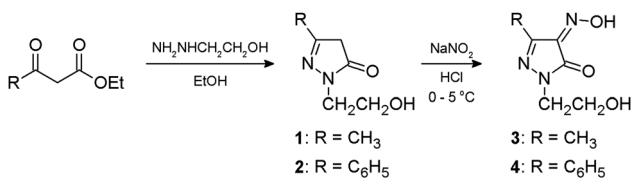

Scheme 1 Synthetic pathway.

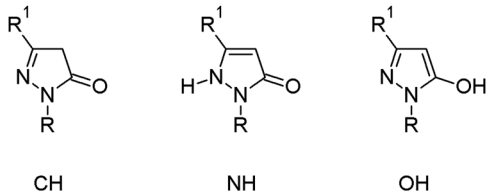

Fig. 1 Tautomeric structures corresponding to compounds **1** and **2**.

Tautomerism is an old issue in pyrazolone chemistry and it has been extensively studied.[18] Since 1-alkyl-5-pyrazolones are less known and considering some results[32,33] showing that small structural variations can have a significant effect on tautomeric equilibria, it is important to discuss the subject in detail considering the data available (the numbering used in the following spectroscopic discussion will be the traditional where N1 is the one bonded to C═O or COH which in turn is C5).

The ^{13}C data for compound **1** in DMSO-d_6, according to the solubility, present a number of signals that agrees with the existence of more than one species in solution. The signals 173.2 and 41.6 ppm can be attributed to a carbonyl at C5 and to a CH_2 at the C4 of the heterocycle. Therefore, it is possible to conclude that the tautomer **CH** (Fig. 1) is present in the solution. On the other hand, the **OH** form accounts the signal at 154.9 ppm that corresponds to an enolic C5, and for another at 86.6 ppm for a vinylic C4 in the heterocycle, as is usual in this solvent.[15,34] However, the presence of the **NH** form cannot be excluded for certain, because of the possibility of a rapid equilibrium between **OH** and **NH** species or the coincidence of the chemical shifts.

The signals for the chain bonded to N1 are duplicated, 59.9 and 58.6 ppm for the CH_2O and 47.7 and 46.1 ppm for the CH_2N. Two signals, attributable to the CH_3 attached to C3 in the heterocycle, are observed at 16.9 and 14.2 ppm. Previous results[15,34] indicate that the **OH** tautomer is the most important in this solvent. Moreover, Holzer[34] showed that the change of the solvent from $CDCl_3$ to DMSO-d_6 has only a very small effect on the chemical shifts of the **OH** form. In this way each signal can be associated with one tautomeric form (Fig. 2). This situation is also valid and it was also used as a guide with the ^1H spectrum, where there are also clues for the presence of mainly two species. A broad singlet, integrating roughly for 1H, at 10.70 ppm is in agreement with the existence of the **OH** (or **NH**) tautomer; this implies that there should be a signal for the vinylic hydrogen, which can be observed at 5.09 ppm. There is also a small broad signal between 4.85 and 4.70 ppm for the CH_2–C═O unit, but in this case integration is not accurate. There are two signals corresponding to CH_3, a singlet with a small shoulder, at 1.99 and 1.98 ppm. Thus, one of the tautomers is present in a larger amount; however, the ratio cannot be determined owing to the overlapping of the signals. In this case, **OH**(**NH**) would be the main specie while **CH** occurs in a tiny amount. It deserves to be noted that the other signals in the proton spectrum are not duplicated, because the differences are not big enough to be observed or the concentration of the minor species is too low.

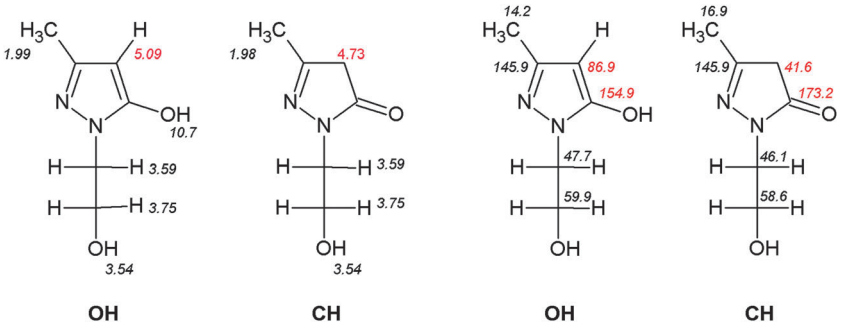

Fig. 2 ^{1}H and ^{13}C NMR chemical shifts of OH and CH tautomers for **1** in DMSO-d_6.

There are two triplets, at 3.75 ppm (2H) for the OCH_2 and 3.59 ppm (2H) for the NCH_2. The signal OH in the chain appears as a singlet (roughly 1H) at 3.54 ppm.

Compound **2** is soluble in chloroform and therefore the NMR spectra were recorded in $CDCl_3$ solution. The ^{13}C spectrum presents a number of signals that shows that only one tautomer occurs in this case. The two key chemical shifts are 172.4 ppm for C5 with a C═O structure and 38.4 ppm for C4 as a CH_2. There is no signal around 80 to 90 ppm for a vinylic carbon, and thus the compound exists largely as the **CH** tautomer. The signal for C3 in the heterocycle has a chemical shift of 155.1 ppm. There are four signals between 125 and 131 ppm, corresponding to the four different carbons of the benzene ring. The signals for the CH_2O and CH_2N can be observed at 61.6 and 47.7 ppm, respectively. The ^{1}H spectrum further supports the existence of the **CH** tautomer alone. The lack of the signals corresponding to OH or NH over 8 ppm and around 5 ppm for the vinylic proton are in agreement with the CH tautomer. The signal for the CH_2 α to the carbonyl can be seen at 3.67 ppm and its area corresponds to 2H. The signals for OCH_2 at 3.97 ppm and NCH_2 at 3.96 ppm are almost completely overlapped; both signals appear as two broad singlets and their area as a whole corresponds to 4H. The ^{13}C spectrum was also recorded in DMSO-d_6, in contrast with the less polar $CDCl_3$, it presents signals showing that only the **OH** tautomer occurs in this case. The two key signals are now 154.3 ppm for C5 with a COH structure and 83.6 ppm for C4 as ═CH. On the other hand, there is no signal around 38 ppm for a saturated C4 in the heterocycle. The signal for C3 can be observed at 148.2 ppm. The corresponding proton spectrum of **2** shows a singlet at 5.73 ppm (1H) for a vinylic CH, and the signal for a CH_2 in C4 (3.67 ppm in $CDCl_3$) is missing; therefore, the equilibrium is shifted to the **OH(NH)** tautomer. The signal corresponding to the OH, however, was not observed. Maybe it is too broad to be detected or a proton–deuterium exchange occurred.

The solid state IR spectrum supports the crystal structure of **1**, when compared with that of **2** it is possible to conclude that a similar tautomer occurs in both cases. Around 3200 to 3300 cm^{-1} can be clearly seen the stretching for the OH of the chain attached to N1. A second peak can be observed around 3120 to 3150 cm^{-1} that can be associated with N–H stretching. There is also a very broad signal starting from 3200 to 1800 cm^{-1} that may also correspond to NH stretching in the heterocycle. Another peak around 1597 cm^{-1} for **1** and at 1586 cm^{-1} for **2** must be assigned to an amidic C═O involved in hydrogen bonding. The C═C stretching is observed at 1548 cm^{-1} for **1** and 1550 cm^{-1} in the case of **2**. Interestingly, in 1-butyl-3-phenyl-5-pyrazolone occurs as the OH tautomer, according to an earlier report.[32]

The most important spectroscopic clue evidencing that the nitrosation reaction took place can be obtained from the fact that the signal for C4 at 86.9 and 41.6 ppm in each tautomer of compound **1** disappears upon reaction. The fundamental tautomeric forms for 1,3-disubstituted-4-nitroso-5-pyrazolones are presented in Fig. 3. Some of the signals in the ^{13}C spectrum of **3** (obtained in DMSO-d_6) are duplicated showing that two species occur in solution. There are two signals for NCH_2 at 46.7 and 46.4 ppm and also two signals for the CH_3 at 17.4 and 12.6 ppm. The signals that can be assigned to C3 and C5 in the heterocycle are also duplicated. In this case the values are 146.3 and 144.4 for C3 and 161.5 and 153.4 ppm for C5. A detailed assignation of the signals was enabled (Fig. 4) based upon the reports by Holzer[16] and Enchev.[17] Moreover, according to these authors, it is possible to consider the existence of one oximino or hydroxyimino tautomer (**NOH** in Fig. 3) with the *E* and *Z* diastereomers in equilibrium (Fig. SI1, ESI†).

The information obtained from the ^{1}H spectrum is also in agreement with the existence of two species in solution. The signal corresponding to the CH_3 is duplicated, at 2.08 and 2.25 ppm. Theoretical calculations[17] showed that, without considering the solvent, the *E* isomer should be more stable in the case of the 1-ethyl homologue. Holzer[16] observed that in DMSO-d_6, the two isomers of 1-phenyl-3-methoxy-4-oximino-5-pyrazolone were equally abundant and he assigned the more deshielded methoxy group to the *Z* isomer and the more shielded to the *E*. Therefore we assigned the signals at 2.25 and 2.05 ppm to the *Z* and *E* diastereomers, respectively; and since they are well

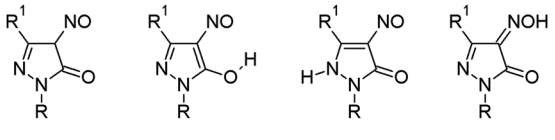

Fig. 3 Main tautomeric forms for 1,3-disubstituted-4-nitroso-5-pyrazolone.

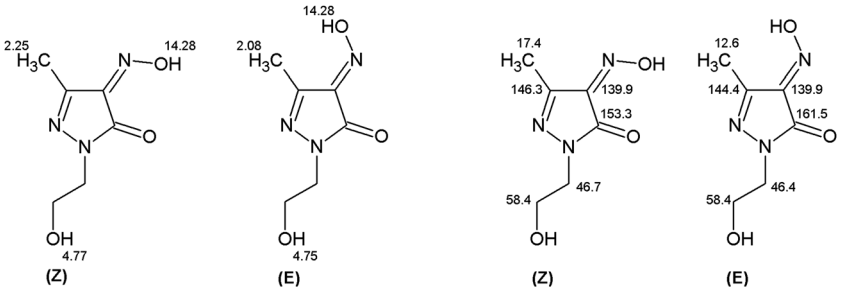

Fig. 4 ^{1}H and ^{13}C NMR chemical shifts corresponding to the diastereomers of compound **3** in DMSO-d_6.

resolved it is possible to estimate the ratio $E:Z$ as 35 : 65. Besides, the proton spectrum shows a signal at 14.28 ppm corresponding to the proton of the hydroxyimino moiety, and a multiplet for 1H, corresponding to the OH in the chain at 4.76 ppm. In this case one triplet for each diastereomer should be expected, but partial overlapping produces a more complex pattern. Two overlapped multiplets with a total area of 4H are observed at 3.55 and 3.63 ppm and they correspond to the two CH_2 in the chain. The less shielded signal should correspond to the OCH_2 unit.

Again, going from **2** to **4**, the signal at 38.4 ppm for C4 in the heterocyclic moiety in the former compound is missing in the ^{13}C spectrum of the latter, showing that the nitrosation reaction was successfully achieved. Regarding the ^{13}C spectrum of **4** (obtained in $CDCl_3$) the data is consistent with only one tautomer. Enchev[17] showed that after considering corrections for the solvent, in chloroform the *Z* isomer of the oximino tautomer becomes more stable. A structure probably stabilized by an intramolecular hydrogen bond. Relevant chemical shifts for the heterocycle are 158.4 ppm for C5 (C═O), 146.8 ppm for C3 (C═N) and 145.7 ppm for C4 (C═NOH). Four signals for the benzene ring between 127.9 and 131.4 ppm are observed and the signals corresponding to the chain are observed at 60.8 (OCH_2) and 47.6 ppm (NCH_2). The ^{1}H NMR spectrum for **4** provides no additional evidence regarding the nature of the tautomers. The signal corresponding to the proton of the ═NOH group is absent, maybe it is too broad to be detected. There is one singlet at 4.00 ppm with an area corresponding to 4H, showing that after nitrosation the two methylenes of the chain became equivalents. It is worthy of note that in the case of **3**, the two CH_2 did not become equivalent, but closer than in compound **1**. This behavior must be a consequence of the electron withdrawing ability of the ═NOH moiety. The benzene ring of compound **4** presents a multiplet from 7.43 to 7.48 ppm for the *m*-H an *p*-H atoms, and therefore it integrates for 3H; the *o*-H atoms present a doublet at 8.07 ppm, each signal with a tiny splitting corresponding to the *m* coupling that it is not measurable. The OH of the chain can be seen as a broad singlet at 2.16 ppm.

The ^{1}H NMR of **4** was also obtained in DMSO-d_6; a broad signal at 14.63 ppm for the ═NOH group can be observed. Besides, two signals in the aromatic region are accompanied by two small ones; this result may be the consequence of the equilibrium between the *E* and *Z* diastereomers of the oxime. Taking this into account, the $Z:E$ ratio would be 90 : 10. It is important to note that the signal corresponding to NCH_2 is not duplicated. Surprisingly the ^{13}C spectrum signals are duplicated just in the case of C1 (128.7 and 128.3) and C4 (130.1 and 129.8) in the benzene ring, and C1 (47.3 and 47.0). Even though this result supports the *E*/*Z* equilibrium, the changes in the chemical shifts going from one diastereomer to the other may be too small or the intensity of some signals is to low, making it impossible to observe more duplicated signals.

Regarding the solid state, IR spectra of compounds **3** and **4** present a signal at 1680 and 1687 cm^{-1}, respectively, that clearly can be assigned to a C═O stretching. A signal that may correspond to C═N stretching of the hydroxyimino group occurs at 1629 cm^{-1} and 1639 cm^{-1}, for **3** and **4**, respectively. The data are in agreement with the crystal structures of these compounds.

Crystal structure descriptions

The crystal structure of **1** consists of isolated molecules engaged in a two-dimensional (4,4) hydrogen bonded grid, which are further connected through a weak CH···π interaction to form a three-dimensional supramolecular network. The clear presence of the H atom in the vicinity of N(2) in the Fourier difference map and the absence of any residual electronic density confirm that compound **1** crystallizes as a pure **NH** tautomer (Fig. 5) and there is not desmotropism as occurs in some 1-phenyl derivatives.[33] The distances around the heterocycle ring (Table 1) correspond to well defined double bonds for C(1)═C(2) and C(3)═O(1), while N(2)–C(1) is clearly a single bond, as expected. This situation is in agreement with previously reported crystal structures for 1-alkyl derivatives.[32]

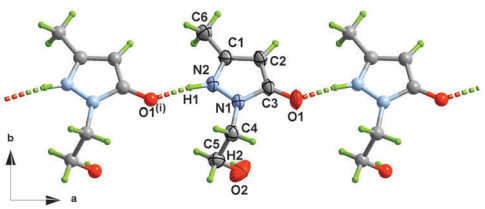

Fig. 5 View of the hydrogen bonded chain in **1** growing along the *a*-axis. Broken lines represent hydrogen bonds. The asymmetric unit has been represented in an ellipsoids model with a 50% probability, together with the atom numbering. Symmetry codes: (i) = $x - 1, y, z$.

Table 1 Selected bond length (Å) in **1**, **3** and **4** compounds

	1	**3**	**4**
N1–N2	1.373(2)	1.406(2)	1.394(3)
N2–C1	1.344(2)	1.292(2)	1.298(3)
C1–C2	1.370(2)	1.457(2)	1.461(4)
C2–C3	1.411(2)	1.497(2)	1.490(3)
N1–C3	1.366(2)	1.348(2)	1.351(3)
C3–O1	1.275(2)	1.228(2)	1.224(3)
C2–N3	—	1.293(2)	1.293(3)
N3–O3	—	1.347(2)	1.359(3)

Each molecule of **1** is connected to other two adjacent ones through the N(2)–H···O(1)^{i} H-bond to build chains [(*i*) = $x - 1$, y, z] (see Table 2 and Fig. 5) running along the *a* axis. These chains are further connected to their adjacent ones through the O(2)–H···O(1)^{ii} H-bond to build the (4,4) grid in the *ac* plane [(*ii*) $x - 0.5$, $-y + 1.5$, $z - 0.5$](Fig. 6a). Therefore, each pyrazolone moiety acts as a double H-bond donor (through the heterocyclic NH and the OH of the hydroxyethyl chain) and as a double H-bond acceptor (through the pyrazolone C=O group). The hydroxyethyl group is torsioned to participate in this H-bond network [N(1)–C(4)–C(5)–O(2) torsion angle being 67.0(2)°] with the O(2) atom far from the heterocycle ring [the separation being 2.457(2) Å]. Within these layers, the heterocycle rings are located above and below the central hydrophilic area, with the methyl groups in the outside of the layer, and a

Table 2 Selected intermolecular interactions for **1**, **3**, and **4** compounds[a–c]

1			
H-bond	D···A (Å)	H···A (Å)	D–H···A (deg)
N(2)–H(1)···O(1)^{i}	2.689(2)	1.76(2)	170(2)
O(2)–H(2)···O(1)^{ii}	2.748(2)	1.90 (3)	167(3)
C–H···π	H···π (Å)	C–H···π (Å)	C–H···π (deg)
C(6)–H(6B)···π(1)^{iii}	2.894(2)	3.536(2)	125.2 (1)
3			
H-bond	D···A (Å)	H···A (Å)	D–H···A (deg)
O(3)–H(3)···O(2)^{iv}	2.628(3)	1.6(1)	170 (5)
O(2)–H(2)···O(1)^{v}	2.740(2)	1.91(4)	163(3)
π···π	C_p···C_p (Å)	β (deg)	γ (deg)
π(2)···π(2)^{v}	3.765(2)	28.96(5)	2.11(7)
4			
H-bond	D···A (Å)	H···A (Å)	D–H···A (deg)
O(3)–H(3)···O(2)^{vi}	2.576(2)	1.84(5)	169(4)
O(2)–H(2)···O(1)^{vii}	2.576(2)	1.68(3)	176(3)
π···π	C_p···C_p (Å)	β (deg)	γ (deg)
π(3)–π(4)^{viii}	3.574(2)	7.95(6)	13.5(1)
C–H···π	H···π (Å)	C–H···π (Å)	C–H···π (deg)
C(9)–H(9)···π(4)^{ix}	3.34(3)	4.100(4)	138(1)

[a] Symmetry codes: (*i*) = $x - 1$, y, z; (*ii*) = $x - 0.5$, $-y + 1.5$, $z - 0.5$; (*iii*) = $-x$, $-y + 2$, $-z + 2$; (*iv*) = $-x + 1.5$, $y + 0.5$, $-z + 1.5$; (*v*) = $x - 0.5$, $-y + 0.5$, $z - 0.5$; (*vi*) = $x + 0.5$, $-y + 0.5$, $z + 0.5$; (*vii*) = $-x + 1.5$, $y + 0.5$, $-z + 0.5$; (*viii*) = x, $-1 + y$, z; (*ix*) = $-x + 2.5$, $y + 0.5$, $-z + 0.5$. [b] Aromatic rings: π(1): N(1)–N(2)–C(1)–C(2)–C(3) for **1**; π(2): N(1)–N(2)–C(1)–C(2)–C(3) for **3**; π(3): N(1)–N(2)–C(1)–C(2)–C(3); π(4): C(6)–C(11) for **4**. [c] D = donor, A = acceptor, H···π = distance between the hydrogen atom of the CH to the centroid of the ring, C_p···C_p = centroid···centroid distance; β = offset angle; γ = angle between mean planes of the rings.

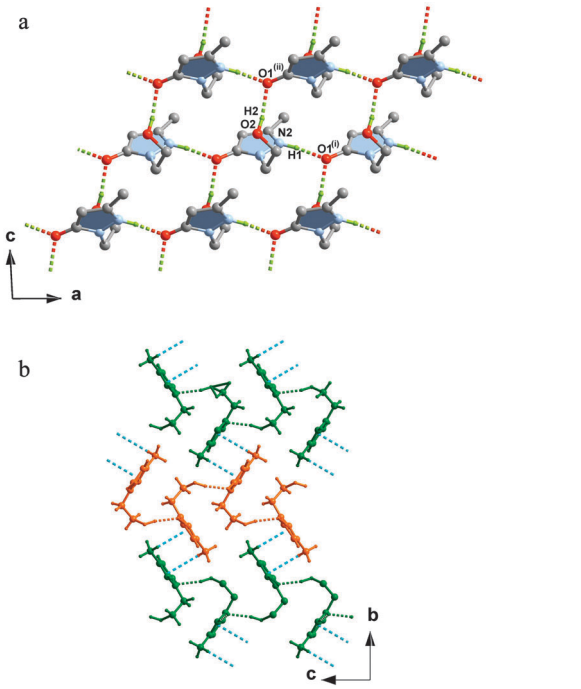

Fig. 6 (a) A view along the *b* axis of the (4,4) hydrogen bonded layer of **1**. The layer grows in the crystallographic *ac* plane. The H atoms are omitted for clarity, except those participating in hydrogen bonds. (b) The crystal packing of **2** viewed along the *a* axis, where each H-bonded (4,4) layer has been depicted in a different colour. The C–H···π interactions are indicated in dashed blue lines. Symmetry codes: (i) = $x - 1$, y, z; (ii) = $x - 0.5$, $-y + 1.5$, $z - 0.5$.

total thickness of *ca.* 9.0 Å. The layers are stacked following an *ABABAB* sequence along the *b* direction. Each layer is engaged with the two adjacent ones, the methyl group forming a weak CH···π interaction with the heterocycle [2.888(1) Å for the H···centroid distance] (Fig. 6b).

The crystal structures of **3** and **4** consist of neutral molecular units which are hydrogen bonded to form a (4,4) layer extended in the (10-1) plane, similar to that of **1**, which are stacked with the methyl and methylene (**3**) or aryl (**4**) groups occupying the interlayer space. The C1=N2 and C3=O1 bond distances in the heterocycle ring of **3** and **4** are shorter than those of **1**; whereas C1=C2 and C2=C3 are longer (see Table 1). These values are in accordance with those of related compounds[35,36] supporting the fact that the prototropic equilibrium is shifted towards the *Z*-diastereomer of the oxime **NOH** (Fig. 3), in solid state.

Each molecule in **3** and **4** participates in four hydrogen bonds, the hydroxyl alkyl and the pyrazolone C=O acting as acceptors and also the hydroxyl alkyl and the hydroxyimino as donors (Fig. 7). The 2D network is formed by the same single H-bond circuit repeated within the layers in **3** and **4**. A total of four molecules participate in the sixteen-atom ring, being ···O–H···O–C–C–N–O–H···O–H···O–C–C–N–O–H···, which exhibit an inversion centre in the middle (see Fig. 8). The H-bonded circuits are almost planar in **3** and **4** [maximum deviation from the mean plane being 0.30(4) Å for H(3) (**3**) and 0.198(2) Å for O(2) (**4**)]. They form an angle with the (4,4) layer of 66.45(4)° for

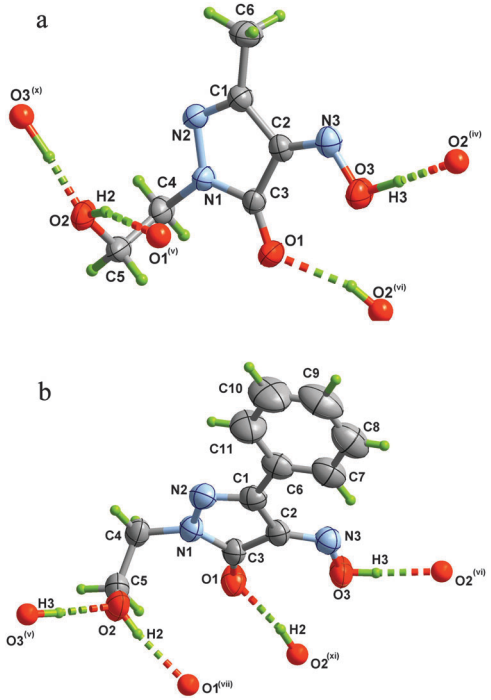

Fig. 7 A view of a fragment of the structures of **3** (a) and **4** (b). The asymmetric units are depicted in an ellipsoids model with a 50% probability, with the atom numbering scheme. Symmetry codes: (*iv*) = $-x + 1.5$, $y + 0.5$, $-z + 1.5$; (*v*) = $x - 0.5$, $-y + 0.5$, $z - 0.5$; (*vi*) = $x + 0.5$, $-y + 0.5$, $z + 0.5$; (*x*) = $-x + 1.5$, $y - 0.5$, $-z + 1.5$, (*xi*) = $-x + 1.5$, $y - 0.5$, $-z + 0.5$.

3 and 55.25(5)° for **4**. These rings are parallel along the *b* axis in **4**, but twisted [with an angle of 79.73(3)°] along the [101] direction; however in **3**, they are twisted along the *b* axis [20.72(1)°] and parallel along the [101] direction (Fig. 8). For the hydroxyl group to participate in this H-bonded pattern the hydroxyethyl substituent exhibits a torsion angle for N(1)–C(4)–C(5)–O(2) of 59.8(3)° (**3**) and 61.30(3)° (**4**), with the hydroxyl group far from the pyrazolone heterocycle [O(2) separation from the mean plane being 2.298(2) (**3**) and 2.362(2) Å (**4**)].

Within the 2D framework of **3** there is also a weak π···π interaction between the heterocycle rings of adjacent molecules in the [101] direction, with a centroid···centroid distance of 3.764(4) Å and an off-set angle of 30.9(2)° (see Table 2). These layers are stacked along the *a* axis in a regular sequence in **3**, with the methyl and the methylene groups occupying the interlayer space. The methyl groups located close to the methylene ones of the neighbouring layer displaying short approach C···C distances in the range 3.665(3)–3.743(5) Å, leading to a distance from the mean planes of adjacent layers of 7.707(3) Å (Fig. 9a). The aryl and the heterocycle rings in the molecular unit of **4** are almost coplanar, with a dihedral angle of 13.6(1)°. Within the (4,4) layer of **4** the aryl ring and the heterocycle of adjacent molecules along the *b* axis exhibit a π···π interaction, with a centroid···centroid separation of 3.573(1) Å and an off-set angle of 7.95(6)°, this short value caused by the restraints of

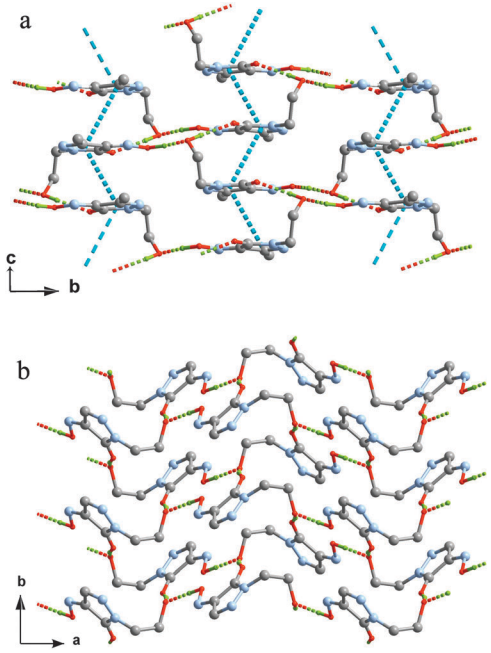

Fig. 8 A view of the (4,4) H-bonded layer growing in the (101) crystallographic plane of **3** (a) and **4** (b). The hydrogen bonds are depicted in dashed red/green lines, whereas the π···π interactions in **3** are presented in blue dashed lines. The H atoms and the aryl ring have been omitted for clarity.

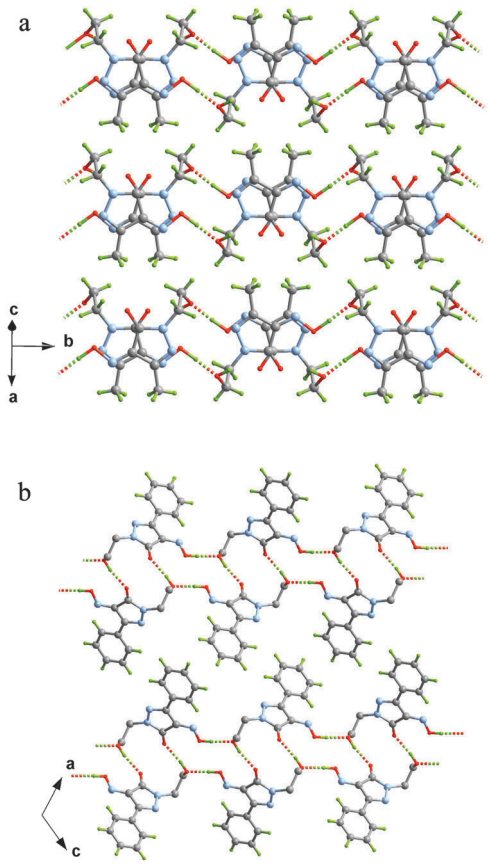

Fig. 9 (a) A view of the crystal packing of **3** where the methyl and methylene groups are occupying the interlayer space. (b) The crystal packing of **4** viewed along the *b* axis. The aryl groups located alternatively above and below each layer occupying the voids of the adjacent one to minimize the interlayer space.

the H-bonding pattern and the interlayer arrangement. The layers are stacked regularly along the *a* axis in **4**, with the aryl groups occupying the interlayer space, alternatively above and below the layer (Fig. 9b). They are located facing the voids of the next layer in order to minimize the interlayer separation, though the separation of the mean planes of adjacent layers is 13.689(2) Å, larger than that of **3**. The aryl groups of adjacent layers are engaged in weak C–H···π interactions [H···centroid separation of 3.347(2) Å].

Conclusions

New hydroxyalkylpyrazolones were synthesized by condensation of two different β-keto esters with 2-hydroxyethylhydrazine. In contrast with previous reports that described alkylation of 3-methyl-5-pyrazolone with primary alkyl bromides, alkylation with halo alcohols turned out to be unsuitable. After nitrosation the 1-(2-hydroxyethyl)pyrazolones afforded two novel oximes. Yields varied from regular in one case to good in the other three.

According to the ^{13}C and ^{1}H NMR data compound **1** in DMSO-d_6 occurs as a mixture of **OH** and **CH** tautomers, the **OH** form is largely the most abundant. On the other hand, compound **2** was studied in $CDCl_3$, the number of signals and the chemicals shift values show that the structure of this derivative corresponds mainly to the **CH** tautomer. In DMSO-d_6, the equilibrium is shifted toward the **OH** tautomer. These results are in agreement with previous reports and show the important role of the solvent.

Compound **3** occurs as a mixture of diastereomeric *E* and *Z* oximes in DMSO-d_6. On the other hand, in $CDCl_3$ **4** also exists as an oximino tautomer, but in this case a single *Z* diastereomer is observed. In DMSO-d_6 there also seems to be a mixture of *E* and *Z* oximes. In both cases (**3** and **4**) in DMSO-d_6 solution the *Z* diastereomer is the most abundant. In spite of the polarity differences between the solvents used, the oxime tautomers proved to be remarkably more stable in both cases.

To the best of our knowledge, this is the first crystallographic description of hydroxyalkylpyrazolones and their corresponding oximes in the literature. The X-ray structure of **1** shows the **NH** tautomer as a predominant structure in solid state. IR data in the solid phase supports the crystal structures and suggest that **2** occurs in a similar tautomer as **1**. The crystallographic data for **3** and **4** shows that the **NOH** are the most important tautomeric structure and the *Z* configuration the most stable so far.

From the supramolecular point of view, the crystal packing of both oximes is similar. The hydrogen bonding networks are mainly responsible for the supramolecular packing, each molecule uses all the donor–acceptor moieties to form layers with similar patterns. The secondary intermolecular interactions are related to the little structural differences between **3** and **4**. The π···π interactions are more important in **4**, whereas the hydrophobic interactions connect the layers in **3**.

Experimental

General remarks

Commercially available reagent grade chemicals were used as received without further purification. Compounds were characterized by FT-IR (Nicolet, Magna 550, KBr pellets), NMR (Bruker Avance 400, 400 MHz for ^{1}H and 100.6 MHz for ^{13}C) were obtained in DMSO-d_6 or $CDCl_3$ according to the solubility, the solvents were used as internal standards, the operating temperature was 28 °C, and the amount of sample used was not weighed neither was the volume of solvent measured. Melting points (°C degrees, Olimpus BX41 microscope plus a Linkam T95-PE temperature controlled stage) are uncorrected. To complete characterization, C, H, and N analyses were carried out (Fisons EA 1108). Chemical shifts for NMR spectra (δ) are quoted in ppm. Infrared values (ν) are quoted in reciprocal centimeters (cm^{-1}).

Synthesis

1-(2-Hydroxyethyl)-3-methyl-5-pyrazolone (1). To a magnetically stirred solution of ethyl acetoacetate (0.5 mol, 65 mL) in 50 mL of ethyl alcohol, 2-hydroxyethyl hydrazine (0.5 mol, 34.5 mL) was dropwise added. The white solid observed two days after the addition was several times crystallized from ethanol. Finally, X-ray quality single crystals in the form of yellow prisms were obtained from the ethanol solution. Yield 55%, mp: 109–111°. Elemental analysis (%): Calc. for $C_6H_{10}N_2O_2$: C, 50.69; H, 7.09; N, 19.71. Found: C, 50.35; H, 7.32; N, 19.37. FTIR (KBr): 3429 (O–H, alkyl chain), 3152 (N–H), 2920 (C–H, sat.), 2936, 2882 (C–H, sat.), 2500–3100 (N–H), 1597 (C═O), 1548 (C═C). ^{1}H-NMR (DMSO-d_6): 10.54 (s, wide, 1H, O–H or N–H, heterocycle), 5.09 (s, 1H, vinylic), 3.75 (t, J = 6.0 Hz, 2H, CH_2O), 3.59 (t, J = 6.0 Hz, 2H, NCH_2), 3.54 (s, 1H, CH_2OH), 1.99 (s, 3H, CH_3). ^{13}C NMR (DMSO-d_6): 172.2 (1C, C-5, C═O), 145.2 (1C, C-3 heterocycle), 86.6 (1C, C-4, vinylic), 59.5 (1C, OCH_2), 47.3 (1C, NCH_2), 13.8 (1C, CH_3).

1-(2-Hydroxyethyl)-3-phenyl-5-pyrazolone (2). The same procedure was followed. Ethyl benzoylacetate (0,47 mol, 81 mL) and 2-hydroxyethylhydrazine (0.47 mol, 32.5 mL) were used. After the addition, the mixture was stirred for one more hour and then filtered. The white solid was crystallized from ethanol several times without affording X-ray quality crystals. Yield: 64.8%, mp: 162–163°. Elemental analysis (%): Calc. for $C_{11}H_{12}N_2O_2$: C, 64.69; H, 5.92; N, 13.72. Found: C, 64.53; H, 6.31; N, 13.36. FTIR (KBr): 3316 (O–H, alkyl chain), 3123 (N–H) 3052 (C–H, unsat.), 2943, 2871 (C–H, sat.), 2500–3100 (N–H, heterocycle), 1586 (C═O), 1550 (C═C). ^{1}H NMR ($CDCl_3$): 7.66 (d–d, J = 4.0 and 8.0 Hz, 2H, phenyl, *o*-), 7.43 (m, 3H, phenyl *m*- and *p*-), 3.97 (s, 2H, CH_2O), 3.96 (s, 2H, NCH_2), 3.67 (s, 2H, CH_2, C-4, heterocycle), 2.69 (s, 1H, OH, alkyl chain). ^{13}C NMR ($CDCl_3$): 158.1 (1C, C-5, C═O), 155.0 (1C, C-3 heterocycle), 131.0, 130.7, 129.1, 125.9 (6C, phenyl), 61.5 (1C, OCH_2), 47.7 (1C, NCH_2), 38.3 (1C, CH_2, C-4, heterocycle). ^{1}H NMR (DMSO-d_6): 7.68 (s, broad, 2H, *o*-), 7.34 (s, broad, 2H, *m*-), 7.24 (s, broad, 1H, *p*-), 5.73 (s, 1H, OH, chain), 3.93 (s, broad, 2H, OCH_2), 3.71 (s, broad, 2H, NCH_2). ^{13}C NMR (DMSO-d_6): 154.3 (1C, C4, heterocycle, COH), 148.2 (1C, C3, heterocycle), 134.7 (1C, C1, benzene), 129.8 (2C, benzene, *o*-), 127.5 (1C, benzene, *p*-), 125.1 (2C, benzene, *m*-), 83.6 (1C, ═CH, C4, heterocycle), 60.1 (1C, OCH_2), 48.8 (1C, NCH_2).

1-(2-Hydroxyethyl)-3-methyl-4-hydroxyimino-5-pyrazolone (3). In a beaker, provided with magnetic stirring and a thermometer, containing 80 mL of ethyl alcohol, compound **1** was dissolved (0.028 mol, 4.0 g) and then concentrated HCl (0.03 mol, 2.4 mL) was added. The mixture was cooled down to 0 °C with a mixture of ice–NaCl. Then a solution of $NaNO_2$ (0.03 mol, 2.13 g) in 8 mL of water is slowly added at such a rate that the temperature remains below 4 °C. Then the mixture was stirred at room temperature for another hour. The solvent was evaporated in a rotary evaporator and the yellow crude was crystallized from a chloroform–EtOH mixture (8 : 2) affording small yellow prisms of sufficient quality for the X-ray diffraction experiments. Yield 74.5%, mp: 165–166°. Elemental analysis (%): Calc. for $C_6H_9N_3O_3$: C, 42.10; H, 5.30, N, 24.55. Found: C, 41.91; H, 5.42; N, 24.48. FTIR (KBr): 3317 (O–H, alkyl chain), 2600–3140 (NO–H,), 1679 (C═O), 1629 (C═N). ^{1}H NMR (DMSO-d_6): 14.28 (s, 1H, N–OH), 4.76 (m, 1H, CH_2–OH), 4.63, 3.55 (m–m, badly resolved, 4H, CH_2–CH_2), 2.25, 2.08 (s–s, 3H, CH_3). ^{13}C NMR (DMSO-d_6): 161.4, 153.5 (2C, C-5, heterocycle, C═O), 146.3, 144.4 (2C, C-3), 139.8 (1C, C-4), 58.4 (1C, OCH_2), 46.7, 46.4 (2C, NCH_2), 17.4, 12.5 (2C, CH_3).

1-(2-Hydroxyethyl)-3-phenyl-4-hydroxyimino-5-pyrazolone (4). The same procedure used to obtain compound **3** was followed. Compound **2** (0.025 mol, 5.0 g), concentrated HCl (0.028 mol, 2.3 mL) and sodium nitrite (0.028 mol, 1.93 g) in 5 mL of water were used. The orange solid was crystallized from a mixture of water–EtOH (9 : 1) yielding deep red block crystals used in the crystallographic measurements. Yield: 79.8%, mp: 168–170°. Elemental analysis (%): Calc. for $C_{11}H_{11}N_3O_3$: C, 56.65; H, 4.75; N, 18.02. Found: C, 56.18; H, 4.71; N, 17.83. FTIR (KBr): 3335 (O–H, alkyl chain), 2600–3100 (O–H, oxime), 1667 (C═O), 1639 (C═N), 1506 (C═C). ^{1}H NMR ($CDCl_3$): 8.07 (d, J = 8.0 Hz, 2H, *o*-), 7.43–7.50 (m, 3H, *m*- y *p*-), 4.02 (s, 4H, CH_2CH_2), 2.16 (s, 1H, OH, chain). ^{13}C NMR ($CDCl_3$): 158.4 (1C, C═O, C-5 heterocycle), 146.8 (1C, C-3, heterocycle), 145.7 (1C, C-4 heterocycle), 131.4, 129.2, 128.8, 127.9 (6C, phenyl), 60.8 (1C, OCH_2), 47.6 (1C, NCH_2).

Crystallography

The data collection for the X-ray diffraction experiment was carried out in an Agilent Supernova diffractometer with Cu radiation (λ = 1.5418 Å) at 293 K for compounds **1**, **3** and **4**. Data were indexed, integrated and scaled with the CrysAlisPRO[37] programs. The crystal structures of **1**, **3** and **4** were solved by direct methods and refined with the full-matrix least-squares technique on F^2 by using the SHELXS-97 and SHELXL-97 programs[38] included in the WINGX[39] software package. All non-hydrogen atoms were refined anisotropically. The hydrogen atoms were set on geometrical positions and refined with a riding model, except those of the hydroxyl group of the ethanol substituent, and those relevant to determine the tautomeric form of the pyrazolone, *i.e.*, the NH in **1**, the NOH in **3** and **4**, which were found in the difference Fourier map and refined isotropically. A summary of the crystallographic data and structure refinement is given in Table 3. The final geometrical calculations and the graphical manipulation were carried out with PARST97[40] and DIAMOND[41] and MERCURY[42] programs, respectively. CCDC numbers 922744–922746 for **1**, **3** and **4**, respectively.†

Table 3 Crystallographic data for compounds **1**, **3** and **4**

	1	**3**	**4**
Formula	$C_6H_{10}N_2O_2$	$C_6H_9N_3O_3$	$C_{11}H_{11}N_3O_3$
FW	142.16	171.16	233.23
Crystal system	Monoclinic	Monoclinic	Monoclinic
Space group	$P2_1/n$	$P2_1/n$	$P2_1/n$
a (Å)	5.7744(3)	8.298(2)	15.8072(7)
b (Å)	15.2403(8)	15.1999(5)	4.9253(2)
c (Å)	7.9988(4)	12.458(3)	16.3792(7)
β (°)	92.736(4)	149.966(3)	116.696(5)
V (Å^3)	703.12(6)	786. 5(3)	1139.27(8)
Z	4	4	4
μ (mm^{-1})	0.855	1.003	0.855
T (K)	293(2)	293(2)	293(2)
ρ_{cal} (g cm^{-3})	1.343	1.446	1.360
λ (Å)	1.54180	1.54180	1.54180
Index ranges	$-6 \le h \le 5$	$-9 \le h \le 9$	$-19 \le h \le 13$
	$-16 \le k \le 18$	$-19 \le k \le 17$	$-5 \le k \le 5$
	$-9 \le l \le 7$	$-14 \le l \le 11$	$-19 \le l \le 19$
Indep. reflect. (R_{int})	1177 (0.0192)	1274 (0.0128)	1626 (0.0299)
Total reflections	1356	1392	2105
Parameters	100	118	167
Goodness-of-fit	0.988	0.996	1.220
R [$I > 2\sigma(I)$]	0.0414	0.0429	0.0378
R_w [$I > 2\sigma(I)$]	0.1059	0.1176	0.1265
R (all data)	0.0470	0.0456	0.0575
R_w (all data)	0.1130	0.1210	0.1325

Acknowledgements

This research was supported by the University of Concepcion (Grant 211023048-10) and also funded by the Ministerio Español de Ciencia e Innovación (Projects CSD2006-00015, MAT2010-16981 and DPI2010-21103-C04-03), and the ACIISI-Gobierno Autónomo de Canarias (Project PIL-2070901). J.P. thanks the funding from the Universidad de La Laguna as part of the Campus of Excellence Project 'CEI Canarias: Campus Atlántico Tricontinental'. P. D.-G. acknowledges the Ministerio Español de Ciencia e Innovación for a FPI predoctoral grant (BES-2011-046637).

Notes and references

1 M. E. Keeney and K. Osseo-Asare, *Coord. Chem. Rev.*, 1984, **59**, 141–201.
2 L. Tschugaeff, *Chem. Ber.*, 1923, **56**, 2083–2522.
3 A. G. Smith, P. A. Tasker and D. J. White, *Coord. Chem. Rev.*, 2003, **241**, 61–85.
4 P. Chaudhuri, *Coord. Chem. Rev.*, 2003, **243**, 143–190.
5 A. I. Buvailo, E. Gumienna-Kontecka, S. V. Pablova, I. O. Fritsky and M. Haukka, *Dalton Trans.*, 2010, **39**, 6266–6275.
6 T. C. Stamatatos, G. Vlahopoulou, C. P. Raptopoulou, V. Psycharis, A. Escuer, G. Christou and S. Perlepes, *Eur. J. Inorg. Chem.*, 2012, 3121–3131.
7 G. N. Schrauzer, *Angew. Chem., Int. Ed. Engl.*, 1976, **15**, 417–426.

8 M. J. Prushan, A. W. Addison, R. J. Butcher and L. K. Thompson, *Inorg. Chim. Acta*, 2005, **358**, 3449–3456.
9 T. W. Greene and P. G. M. Wuts, *Protective Groups in Organic Synthesis*, Wiley, Toronto, 2003, pp. 355–358.
10 J. Charalambous and M. J. Kensett, *Inorg. Chim. Acta*, 1976, **16**, 213–217.
11 G. Ivanova and V. Enchev, *Chem. Phys.*, 2001, **264**, 235–244.
12 V. Enchev, G. Ivanova and N. Stoyanov, *J. Mol. Struct. (THEOCHEM)*, 2003, **640**, 149–162.
13 L. Knorr, *Ber. Dtsch. Chem. Ges.*, 1884, **17**, 2032–2049.
14 J. Bartulin, J. Belmar, H. Gallardo and G. Leon, *J. Heterocycl. Chem.*, 1994, **31**, 561–563.
15 J. Belmar, J. Alderete, M. Parra and C. Zuñiga, *Bol. Soc. Chil. Quim.*, 1999, **44**, 367–374.
16 W. Holzer and L. Hallak, *Heterocycles*, 2004, **63**, 1311–1334.
17 V. Enchev and S. Angelova, *J. Mol. Struct.*, 2009, **897**, 55–60.
18 W. Holzer, C. Kautsch, C. Laggner, R. M. Claramunt, M. Pérez-Torralba, I. Alkorta and J. Elguero, *Tetrahedron*, 2004, **60**, 6791–6805.
19 P. Zhang, Z. Wang, M. Xie, W. Nie and L. Huang, *J. Chromatogr., B: Anal. Technol. Biomed. Life Sci.*, 2010, **878**, 1135–1144.
20 C. Ding, L. Wang, C. Tian, Y. Li, Z. Sun, H. Wang, Y. Suo and J. You, *Chromatographia*, 2008, **68**, 893–902.
21 J. S. Casas, M. García-Tasende, A. Sánchez, J. Sordo and A. Touceda, *Coord. Chem. Rev.*, 2007, **251**, 1561–1589.
22 F. Marchetti, C. Pettinari and R. Pettinari, *Coord. Chem. Rev.*, 2005, **249**, 2909–2945.
23 S. Umetani, *J. Alloys Compd.*, 2006, **408–412**, 981–984.
24 R. Bianchini, M. Bonanni, M. Corsi and A. S. Infantino, *Tetrahedron*, 2012, **68**, 8636–8644.
25 W. Herbst and K. Hunger, *Industrial Organic Pigments: Production, Properties Applications*, Wiley-VCH Verlag, Weinheim, 3rd. edn, 2004, pp. 601–636.
26 X. Qi, Y. Okuna, T. Hosoi and Y. Nomura, *J. Pharmacol. Exp. Ther.*, 2004, **311**, 388–393.
27 S. A. Abdel-Latif, O. M. El-Roudi and M. G. K. Mohamed, *J. Therm. Anal. Calorim.*, 2003, **73**, 939–950.
28 L. Beverina, M. Crippa, M. Sassi, A. Monguzzi, F. Meinardi, R. Tubino and G. A. Pagani, *Chem. Commun.*, 2009, 5103.
29 S. A. Latif and Y. M. Issa, *Nat. Sci.*, 2010, **2**, 1035.
30 J. Bartulin, J. Belmar and G. Leon, *Bol. Soc. Chil. Quim.*, 1992, **37**, 13–18.
31 G. Varvounis, Y. Fiamegos and G. Pilidis, *Adv. Heterocycl. Chem.*, 2001, **80**, 73–156.
32 J. Belmar, C. Jiménez, C. Ruiz-Pérez, F. S. Delgado and R. Baggio, *Acta Crystallogr., Sect. C: Cryst. Struct. Commun.*, 2006, **62**, o599–o601.
33 C. Foces-Foces, C. Fontenas, J. Elguero and I. Sobrados, *An. Quim. Int. Ed.*, 1997, **93**, 219–224.
34 B. M. T. Wolf, W. G. Eller and W. Holzer, *Heterocycles*, 2008, **75**, 2035–2042.
35 J. Belmar, C. Jiménez, L. Ortíz, M. T. Garland and R. Baggio, *Acta Crystallogr., Sect. C: Cryst. Struct. Commun.*, 2006, **62**, o76–o78.
36 J. Belmar, F. R. Pérez, Y. Moreno and R. Baggio, *Acta Crystallogr., Sect. C: Cryst. Struct. Commun.*, 2004, **60**, o705–o708.
37 Agilent, CrysAlis PRO. Agilent Technologies UK Ltd, Yarnton, England, 2011.
38 G. M. Sheldrick, *Acta Crystallogr., Sect. A: Found. Crystallogr.*, 2008, **64**, 112–122.
39 L. J. Farrugia, *J. Appl. Crystallogr.*, 1999, **32**, 837(WINGX).
40 M. Nardelli, *J. Appl. Crystallogr.*, 1995, **28**, 659.
41 DIAMOND 2.1d, Crystal Impact GbR, CRYSTAL IMPACT, K, Brandenburg & H. Putz GbR, Bonn, Germany, 2000.
42 Mercury: visualization and analysis of crystal structures C. F. Macrae, P. R. Edgington, P. McCabe, E. Pidcock, G. P. Shields, R. Taylor, M. Towler and J. van de Streek, *J. Appl. Crystallogr.*, 2006, **39**, 453.

